Open Archive Toulouse Archive Ouverte

OATAO is an open access repository that collects the work of Toulouse researchers and makes it freely available over the web where possible

This is an author's version published in: https://oatao.univ-toulouse.fr/22319

To cite this version:

Lucciardi, Jean-Alain and Thomas, Nathalie and Boucheret, Marie-Laure and Poulliat, Charly and Mesnager, Gilles *Receiver for FTN Signaling in Non-Linear Channel: Joint Channel Estimation and Synchronization.* (2017) In: 28th IEEE International Conference on Personal, Indoor and Mobile Radio Communications (PIMRC 2017), 8 October 2017 - 13 October 2017 (Montreal, Quebec, Canada).

Any correspondence concerning this service should be sent to the repository administrator: tech-oatao@listes-diff.inp-toulouse.fr

Receiver for FTN Signaling in Non-Linear Channel: Joint Channel Estimation and Synchronization

Jean-Alain Lucciardi*, Nathalie Thomas[†], Marie-Laure Boucheret[†], Charly Poulliat [†] and
Gilles Mesnager*
* Embedded Systems, IRT Saint-Exupery, Toulouse, France
Email: forename.name@irt-saintexupery.com
[†]University of Toulouse, INPT-ENSEEIHT/IRIT, Toulouse, France
Email: forename.name@enseeiht.fr

Abstract—In order to increase the capacity of future satellite communication systems, faster-than-Nyquist (FTN) signaling is increasingly considered. The gain in terms of transmission rate is obtained at the price of significant intersymbol interference (ISI) introduction. To benefit from an improved spectral efficiency (SE), m any iterative detectors have already been investigated, demonstrating the interest of such a waveform in linear and non linear channels. A thorny point in FTN signaling remains its synchronization since the usual algorithms considered in the DVB-S2X standard cannot be applied on this waveform without significant l oss o n t he p erformance. T his paper proposes a synchronization scheme for FTN signaling in a satellite context. It is based on a Volterra decomposition of the received signal in order to fit b oth w ith l inearized and non-linearized amplifiers which can be found in the satellite payload. Two steps, initialization and tracking are considered, based on training sequences fulfilling t he DVB-S2Xs frames requirements. After start of sequence detection and frequency offset correction, the channel estimation is used for time offset issue in the two proposed schemes. Their performance are compared to the performance of a perfect synchronized detection.

I. Introduction

FTN signaling was first c onsidered b y M azo i n [1], increasing the transmission rate of binary symbols with a cardinal sine pulse shaping. He has shown that above a compression factor, usually called *Mazo limit*, the ISI does not decrease the minimum euclidean distance and so, the theoretical Bit Error Rate (BER) achievable for the binary transmission. This study opened the door to a similar investigation considering usual root raised cosine (RRC) filters, g iving e quivalent c ompression limits depending on the roll-off factor [2].

However, the introduced ISI requires the implementation of advanced receivers. The best performance is offered by Maximum a Posteriori (MAP) detectors [3], but lower complexity receivers as minimum mean squared error (MMSE) or Colavolpe's detector [6] perform well. Therefore, in order to benefit from an im-

proved capacity, iterative detection, also called turbo-equalization/detection, is advocated with reduced order modulations. When linear channel is considered, the satellite communications'efficiency can be improved as underlined in [4].

Furthermore, the payload can introduce non-linear distortions, the channel can then be approximated by Volterra series as depicted by Benedetto in [5]. Employed for Nyquist signaling in the saturation regime, iterative non-linear detection based on Volterra kernels suggests interesting performance in [6].

Since non-linear channel requires advanced receivers, allowing FTN signaling in the saturation regime makes sense. Indeed, the ISI due to both the payload and the FTN signaling can be equalized within a joint model. In [7], the interest of such a signaling is demonstrated, supported by the study in [8] which highlighted the robustness of the FTN waveform in non-linear channel. Iterative MAP detection is implemented in the following of this paper.

The issue of signal synchronization has to be addressed. Usual algorithms depicted in [9] for timing recovering (Gardner's approach) and frequency recovering (Luise and Regiannini's approach) are not suitable in strong ISI context. In [10], a synchronization scheme for FTN signaling in DVB-S2 background is considered. The performance depicted differs when linear or non-linear channel transmission are considered since the non-linear distortion is not taken into account in the derivation of the proposed algorithm. Moreover the acquisition mode depicted in [10] considers joint maximum likelihood (ML) estimation of both the timing error and the frequency offset, and thus, this method requires high computational load. In [11], a well performing non data-aided (NDA) method is proposed for frequency offset estimation of FTN signaling. The high performance achieved by in [11] has to be balanced with the considered model. The considered channel is

indeed a linear one, thus the non-linear regime is not addressed. Moreover, the method considers in advance a perfect time synchronization whereas this assumption is not obvious for synchronization matters. Moreover, in [10] and [11], no channel estimation is investigated whereas the detection can be improved with a time-variant equalization model as highlighted in this paper.

In this paper, we investigate the performance of joint synchronization and channel estimation for FTN signaling. It will be illustrated in DVB-S2X context. The proposed synchronization scheme operates in two main steps: A first one called *INITIALIZATION STEP* is performed over a dummy frame (DF) as it is generally defined in standard guidelines [12]. This step performs timing recovering paired with Volterra's kernels estimation [14]. The frequency recovering is based on Morelli and Mengali's frequency offset estimation [15] for strong ISI signaling. The second step is called *TRACKING STEP* and is performed on the PLHeader's start of frame (SOF) and Pilots inserted in the data flow as defined in the standard [12]. The interest of channel estimation for detection with no sampling correction is investigated, leading to potential gains.

The paper is organized as follows. Section II briefly reviews the end-to-end FTN signaling system in the non-linear context and the associated channel estimation is addressed. Section III consists of the description of *INITIALIZATION* and *TRACKING* steps of the proposed synchronization scheme. Section IV gives the performance of the different investigated algorithms. Conclusions are given in Section V.

II. FASTER-THAN-NYQUIST SIGNALING IN NON-LINEAR CHANNEL - DESCRIPTION AND MODEL ESTIMATION

A. Channel model and notations

At the transmitter side, the binary data u_k is encoded into a codeword c_k using low-density parity-check (LDPC) error-correcting codes of coding rate ρ. The data interleaving is followed by the bit mapping into complex symbols $a_k, k \in \mathbb{Z}$ belonging to a M-ary phase shift keying (PSK) constellation with a Gray mapping. FTN signaling consists of a symbol rate acceleration w.r.t. the Nyquist rate: $R_s = \frac{1}{T_s} = \frac{1}{\alpha T}$ with T-orthogonal root raised cosine (RRC) filter $h(t)$. β denotes the shaping filter's roll-off factor. The compression factor of the FTN transmission is $\alpha \in [0, 1]$. The baseband transmitted signal is

$$x_e(t) = \sum_k a_k h(t - k\alpha T) \qquad (1)$$

The non-linear distortions are introduced to (1) by the satellite payload, acting as a transparent repeater (see Figure 1). In this paper, the allocated transponder's bandwidth for transmission is $B = 40$MHz. Since the shaping filter $h(t)$ is designed so that $BT \simeq 1 + \beta$ and

considering that the roll-off is $\beta = 0.1$ in the following of this paper, the symbol rate R_s is equal to $\frac{36}{\alpha}$MBauds for the transmission.

Since we consider a single carrier scenario, the input multiplexer (IMUX) and output multiplexer (OMUX) act as linear filters on both sides of the high power amplifier (HPA). When operated in the saturation regime, the payload introduces strong non-linear ISI, compromising even more the synchronization of the FTN signal.
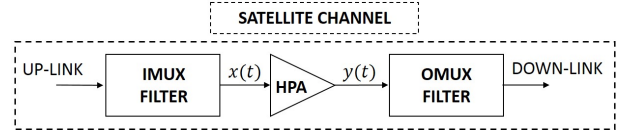

Fig. 1. Transparent satellite payload

In Figure 2 the AM/AM curve of the considered HPA gives the output back-off (OBO) as a function of the input back-off (IBO). The considered amplifier matches with a Saleh model [19] with parameters $\alpha_s = 2.1587$ and $\beta_s = 1.1517$ such as :

$$|y| = \frac{\alpha_s |x|}{1 + \beta_s |x|^2} \qquad (2)$$

where x and y are respectively the signals at the HPA input and output. The 1dB compression point on the figure highlights the saturation regime of the amplifier.

Finally, on the downlink an additive white Gaussian noise (AWGN) is added to the signal. In the following, $2N_0$ denotes the power spectral density of the complex channel noise. The received noisy signal is filtered with the filter $h_r(t) = h^*(-t)$, where $(.)^*$ denotes the complex conjugate, matching the shaping filter $h(t)$ and resulting in a colored sampled noise n_k.
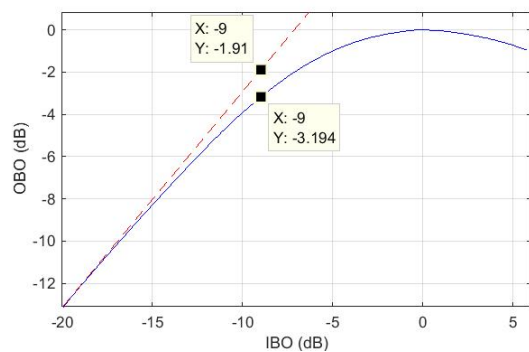

Fig. 2. OBO Vs IBO - AM/AM curve of a conventional HPA

The non-linear channel model with Volterra's series was first proposed by Benedetto et. al. in [5]. It consists of a polynomial decomposition of the non-linear amplification with only odd coefficients.

$$|y| = \sum_k \gamma_{2k+1} |x|^{2k+1} , \qquad (3)$$

where γ_{2k+1} are the Volterra decomposition's coefficients. Then, the non-linear channel is depicted by both linear and non-linear terms. Here the model is truncated to the third order Volterra kernels of which optimization is obtained for the 7th order polynomial decomposition in (3). The discrete received signal is given by

$$r_k = \sum_l a_{k-l}K_l + \sum_m \sum_n \sum_p a_{k-m}a_{k-n}a_{k-p}^* \\ K_{m,n,p} + n_k \quad (4)$$

where K_l and $K_{m,n,p}$ respectively represent the 1st and 3rd order Volterra kernels. This model is used for the trellis based MAP detection [18]. The trellis is computed with a truncated non-linear channel length L, with L 1st order Kernels and 3^L 3rd order kernels. The MAP is then used in an iterative turbo-detection sheme depicted in Figure 3, using a LDPC soft decoder based on Belief Propagation (BP) decoder.
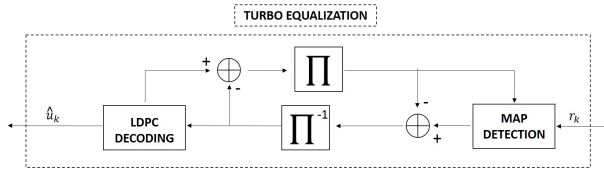

Fig. 3. Turbo-equalization

When a Volterra model is considered, the difference between Nyquist and FTN signaling lies in the fitting and amplitude of the kernels and thus, the channel selectivity. In the following of this paper, the signal to noise ratio (SNR) means C/N, the ratio between the total carrier power and the white Gaussian noise power in the bandwidth B.

Figure 4 sums-up the global transmission scheme when perfect synchronization is considered.
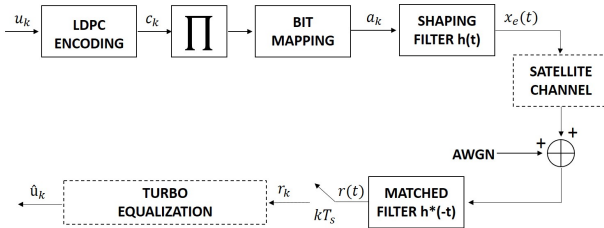

Fig. 4. Transmission channel scheme

A key point of the considered detection scheme has to be briefly discussed here. In Figure 4, the filter considered at the receiver side is a partial matched filter which only matches the shaping filter $h(t)$. In this paper, the considered model differs from the proposed model in [7] of which the filter at the receiver matches a reduced Volterra model taking into account the whole channel. By so doing, their model leads to a linear channel allowing detection on an Ungerboeck model [16]. In

contrast, our channel model is not symmetric and not causal making Ungerboeck model unfeasible. The MAP detection in this paper considers a branch metric in the BCJR algorithm of type Forney [17] without whitening filter and so neglecting the noise correlation in the model:

$$\gamma_t(m', m) \propto |r_k - (\sum_l a_{k-l}K_l + \sum_m \sum_n \sum_p a_{k-m} \\ a_{k-n}a_{k-p}^* K_{m,n,p})|^2 + 2N_0 ln P(a_k) \quad (5)$$

This choice is motivated by two key aspects:
- For an Ungerboeck model, a perfect symmetry of the channel is mandatory. Then, the sensitivity to timing error is detrimental.
- The required filter at the receiver detailed in [6] for Ungerboeck model has to be modified when the IBO and/or the compression factor α are modified. In [7], the compression factor is fixed for each modulation in order to decrease the complexity of the receiver. The transmission does not benefit from an improved granularity of the joint Modulation and Coding (ModCods) and compression factor combination as the model implemented in this paper.

B. Non-linear channel estimation

Here, the channel estimation relating to the non-linear model (4) is briefly investigated and consists of the 1st and 3rd order Volterra kernels estimation. A least-squares-type method is considered in [14] based on a training sequence $s = [s_1, ..., s_N]$ of length N. The pattern of the training sequence is not discussed here but in the following section. In [14] - Section IV, Morgan et. al. give the following least-squares solution

$$\tilde{K} = (S_c^H S_c)^{-1} S_c^H y, \quad (6)$$

where y is a length N block of the received training sequence sent through the channel. S_c denotes a $L_{tot} \times (N - L_{tot})$ circulant matrix build from the training sequence s such that $[S_c]_{i,j} = s_{|i+j-1|_N}$ where $|i+j-1|_N$ means "$|i+j-1|$ modulo N". $\tilde{K}$ is a vector of length L_{tot} containing L estimated 1st order Kernels and L_3 estimated 3rd order kernels, with $L_3 = L_{tot} - L$. The channel estimation performance is discussed in Section IV-A.

III. FTN SYNCHRONIZATION

In this Section, time and frequency offsets correction is considered for FTN signaling in a non-linear channel. We first review the time and frequency offset estimation based on a training sequence compliant with the DVB-S2X standard for *INITIALIZATION STEP*. Secondly, two methods are discussed for timing estimation. The third subsection highlights the changes of algorithms to be suited to *TRACKING STEP*. Finally, the architecture of the receiver for both *INITIALIZATION STEP* and *TRACKING STEP* is depicted in Figure 8.

Here is briefly detailed the different impairments to be taken into account for synchronization issue:

- First, δ_T is the sampling instant offset. Regarding (4), we consider now $r_{k+\delta_T} = r(kT_s + \delta_T)$. There is no value restriction for this offset, $\delta_T \in [-\frac{T_s}{2}, +\frac{T_s}{2}]$.
- For DTH broadcasting services, the maximum carrier frequency instability considered in the standard is $\delta_f = \pm 5$MHz [13], according to the ESA channel model. In this paper, $\frac{\delta_f}{R_s} < 15\%$ is considered.
- The phase noise ϕ_k considered in the following comes from the "Digital synthesis of the phase noise in simulations" appendix of the DVB-S2X guidelines [13].

Therefore , the sampled received signal to be synchronized after matched filtering is

$$r'_k = r_{k+\delta_T}e^{j(2\pi k\frac{\delta_f}{R_s}+\phi_k)} + n_k, \qquad (7)$$

Note that the synchronization algorithm depicted in the following does not need oversampling factor as in Gardner detection [9].

A. Start of sequence (SOS) detection over a dedicated dummy frame - Initialization step

The standard DVB-S2X offers the possibility to generate Dummy frames with arbitrary content [12]. We propose indeed a training sequence build among a dummy frame of N=3330 symbols. More specifically, the start of frame (SOF) pattern of L_s=26 $\pi/2$-BPSK symbols located in the PLHeader is periodically repeated N_s=128 times. Considering the repeated training sequence $s = [s_1,...,s_{26}]$ and knowing the channel components, the expected distorted signal at Nyquist sampling instant is

$$\tilde{s}_k = \sum_l s_{k-l}K_l + \sum_m \sum_n \sum_p s_{k-m}s_{k-n}s^*_{k-p}K_{m,n,p} \qquad (8)$$

Then, a correlation is performed on the sampled received signal with $\tilde{s}$ for the SOS detection

$$\lambda(r'_k, \tilde{s}) = \left| \sum_{l=0}^{\frac{L_s}{2}-1} \tilde{s}_l^* r'_{k+l} \right|^2 + \left| \sum_{l=\frac{L_s}{2}}^{L_s-1} \tilde{s}_l^* r'_{k+l} \right|^2 \qquad (9)$$

The received signal r'_k is sampled with the time offset δ_T which is not taken into account into $\tilde{s}$, the mismatch does not avoid the sequence detection. In Figure 5, the start of each repeated sequence is detected despite the low considered OBO and SNR and the time offset δ_T. Considering the frequency offset requirements, the half of the training sequence is short enough.

B. Frequency offset estimation over a dedicated dummy frame - Initialization step

Once the SOS is achieved, a coarse frequency offset estimation is applied. With this in mind, we considered the proposed methods in [15] for frequency
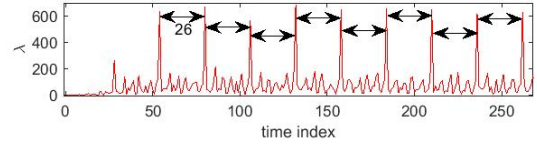

Fig. 5. Start of sequence detection by correlation - SNR = 3dB - OBO = 1dB - $\frac{\delta_f}{R_s}$=5% - α = 0.7, β = 0.1

offset estimation in strong ISI transmission context. More specifically, we investigate the proposed algorithm named "MLE#2" in [15] since our training sequence fits with their periodic training sequence requirement. The estimated $\frac{\delta_f}{R_s}$, noted $\widehat{\nu}$, is given by:

$$\widehat{\nu} = \frac{1}{2\pi L_s}arg\left(\frac{1}{(N_s-1)} \sum_{j=1}^{N_s-1} \sum_{k=j.L_s}^{(j+1)L_s} r'_k r'^*_{k-L_s} \right) \qquad (10)$$

A first coarse frequency offset estimation and correction is applied, ensuring a new $\frac{\delta_f}{R_s} < 1.10^{-3}$ in the worst case of SNR/OBO (3dB/1dB). Then a more accurate estimation/correction based on a larger sequence can be applied. The training sequence remains the same dummy frame depicted previously but the periodicity taken into account differs: We now consider L_s=260 symbols repeated N_s=12 times. The resulting frequency estimation is more accurate since in the worst case of SNR/OBO, a precision of 9.10^{-5} on $\frac{\delta_f}{R_s}$ is achieved. The whole performance of the frequency offset estimation is depicted in Section IV-A.

C. Sampling methods and corresponding detectors - Initialization step

Once the frequency offset correction is achieved, the timing estimation and correction is performed using to the non-linear channel estimation depicted in paragraph II-B. The channel estimation leads to two different receivers, a first scheme without timing correction (Scheme A) and a second scheme with timing correction (Scheme B). We consider a residual frequency offset ϵ_f in the received signal (7) after the frequency offset correction. The considered signal model is:

$$\tilde{r_k} = r_{k+\delta_T}e^{j(2\pi k\epsilon_f+\phi_k)} + n_k, \qquad (11)$$

Note that $r_{k+\delta_T}$ is the sampled Volterra model with time offset:

$$r_{k+\delta_T} = r(kT_s + \delta_T) = \sum_l a_{k-l}K_{l+\delta_T} + \sum_m \sum_n \sum_p a_{k-m}a_{k-n}a^*_{k-p}K_{m,n,p+\delta_T} \qquad (12)$$

where $K_{l+\delta_T}$ and $K_{m,n,p+\delta_T}$ respectively represent the 1st and 3rd order Volterra kernels of the channel when sampled with the inherent δ_T sampling offset of (7).

So, the channel estimation (6) resulting of the sampled received signal (11) is

$$\tilde{\boldsymbol{K_{\delta_T}}} = (\boldsymbol{S_c}^H \boldsymbol{S_c})^{-1} \boldsymbol{S_c}^H \tilde{\boldsymbol{r}}, \qquad (13)$$

where $\tilde{\boldsymbol{r}}$ is the received signal associated to the dummy frame of N=3330 known symbols sent through the channel. $\boldsymbol{S_c}$ denotes a $L_{tot} \times (N - L_{tot})$ circulant matrix build on the dummy frame $\boldsymbol{s} = [s_1, ..., s_{3330}]$.

From there, two different receiver schemes are considered.

1) Scheme A - Trellis update without time offset correction: Taking into account the estimated channel $\tilde{\boldsymbol{K_{\delta_T}}}$, the trellis used for MAP detection is updated so that the considered model is (13). In the BCJR algorithm, the branch metric is updated in the following manner:

$$\gamma_t(m', m) \propto |r_k - (\sum_l a_{k-l} K_{l+\delta_T} + \sum_m \sum_n \sum_p a_{k-m}$$
$$a_{k-n} a_{k-p}^* K_{m,n,p+\delta_T})|^2 + 2N_0 ln P(a_k) \qquad (14)$$

In this case there is no extra timing correction since the detection model is designed for the channel including the time offset. This scheme A offers a perfect match of the received signal sampling instant and the model, on the contrary of the following scheme B.

2) Scheme B - Time offset correction: We first define a matrix $\boldsymbol{K^{(1)}}$ of size $\chi \times L$. Each line of $\boldsymbol{K^{(1)}}$ contains the theoretical pre-computed 1st order kernels with pre-defined offset timing $\Delta_T = [-\frac{\chi-1}{2(\chi+1)}T_s, ..., -\frac{1}{\chi+1}T_s, 0, +\frac{1}{\chi+1}T_s, ..., +\frac{\chi-1}{2(\chi+1)}T_s]$. The timing offset measure consists in the minimization of distance D as a function of $i = [1, \chi]$:

$$D = |\boldsymbol{K^{(1)}_{i,[1,L]}} - \tilde{\boldsymbol{K_{\delta_T}}}|^2 \qquad (15)$$

Estimate $\widehat{\delta_T}$ of δ_T is set to $\Delta_T(i)$, the sampling offset is used for timing correction. The MAP detection is then implemented with the theoretical Volterra kernels in (4). Considering the MAP detection, the loss due to a timing error of $0.05T_s$ is 0.1dB. It has motivated the choice of the value $\chi = 19$ resulting in a time step $T_s/20$ in $\boldsymbol{K^{(1)}}$.

The relevance of each scheme and associated performance are discussed in Section IV-B.

D. Tracking step - Reuse of the previous estimators

During the transmission, frequency and timing corrections are achieved ensuring reliable detection. As a reminder, we briefly depict the recommended Pilot structure frame in [12]. The preamble PLHeader (PLH) is composed of the SOF sequence followed by 64 symbols of PLSCODE. Moreover, a Pilot sequence of N_P=36 known symbols is inserted every N_D=1440 data symbols.

- The SOF detection used for *INITIALIZATION STEP* is reused in the *TRACKING STEP*. An additional Pilot detection is needed. It is achieved thanks to a

correlator similar to (9) with $\boldsymbol{p} = [p_1, ..., p_{36}]$ and its corresponding expected $\tilde{p}$ based on the known Pilot sequence at the output of the Volterra based channel:

$$\lambda(r_k', \tilde{p}) = \left| \sum_{l=0}^{\frac{L_s}{2}-1} \tilde{p_l}^* r_{k+l}' \right|^2 + \left| \sum_{l=\frac{L_s}{2}}^{L_s-1} \tilde{p_l}^* r_{k+l}' \right|^2 \qquad (16)$$

- The frequency offset estimation is realized on two consecutive Pilot sequences with Menagli's method:

$$\widehat{\nu} = \frac{1}{2\pi(N_D + N_P)} arg \left(\sum_{k=k_0}^{k_0+N_P-1} r_k r_{k-N_D}^* \right) \qquad (17)$$

where k_0 is the index of the first symbol of the received Pilot. The frequency offset is estimated and corrected each received Pilot by considering the two last consecutive received Pilots. The performance of the frequency offset tracking is discussed in Section IV-A. The frequency drift, reported in the ESA channel model, is 30KHz/s according to [13].

- The channel estimation during tracking is applied on each PLH detected thanks to the SOF detector:

$$\tilde{\boldsymbol{K_{\delta_T}}} = (\boldsymbol{S_c}^H \boldsymbol{S_c})^{-1} \boldsymbol{S_c}^H \tilde{\boldsymbol{r}}, \qquad (18)$$

where $\tilde{\boldsymbol{r}}$ is the received samples corresponding to the PLH of N=90 known symbols sent through the channel. $\boldsymbol{S_c}$ denotes a $L_{tot} \times (N - L_{tot})$ circulant matrix build on the PLH $\boldsymbol{s} = [s_1, ..., s_{90}]$. In [13], the time drift to take into account for standard requirements corresponds to 100 p.p.m.

In Scheme A, the trellis used for detection can be updated on each received start of frame on which the channel estimation is applied. For Scheme B, during *TRACKING STEP*, the time offset correction is the same as during *INITIALIZATION STEP*, as depicted in Figure 8. The frequency of correction based on SOF is high enough considering a 100 p.p.m. drift.

The performance of the different estimators and the detection of schemes A and B are discussed in the following section.

IV. RESULTS

In this section, we first analyse both the channel and the frequency offset estimations, for both the *INITIAL-IZATION STEP* and the *TRACKING STEP*. Secondly, the degradation due to both synchronization schemes A and B is highlighted and compared to an ideal synchronized signaling. The degradation is computed taking into account the whole synchronization impairments described in III during both *INITIALIZATION STEP* and *TRACKING STEP*.

A. Estimators performances

We consider training sequences of $N = 3330$ and $N = 90$ known symbols, respectively the Dummy frame length and the PLHeader length. The robustness of the channel estimation as a function of the SNR is not discussed since it performs similarly from 0dB to 20dB. In Figure 6, the impact of input back-off (IBO) on the estimation relevance is depicted considering the mean squared error (MSE) between the theoretical and the estimated kernels. The truncation takes into account L=21 1st order kernels and the $L_{tot}-L$=100 most powerful 3rd order kernels for both estimated and theoretical model. SNR is fixed to the worst case of 3 dB.
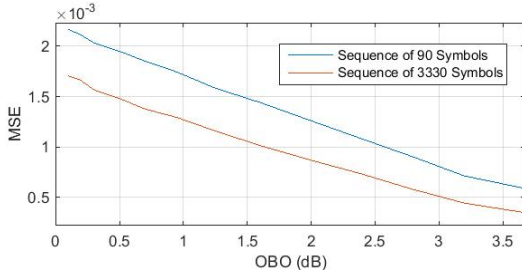

Fig. 6. MSE between theoretical and estimated sets of 1st and 3rd order kernels as a function of the IBO with training sequence length 3330 (DF) and 90 (PLHeader) - $\alpha = 0.7$, $\beta = 0.1$ and SNR = 3 dB - Monte-Carlo on 1000 Dummy Frames / 1000 PLHeader.

The lower the back-off is, the higher the ISI and then the higher the MSE are. Obviously, the estimation performs better when a longer training sequence is adopted but based on PLH, the estimation is accurate enough for detection.

The frequency estimation performance is investigated for *INITIALIZATION STEP* estimator (10). First, the coarse frequency offset estimation error $\epsilon_c = |\widehat{\nu} - \frac{\delta_f}{R_s}|$ is computed as a function of SNR with an initial value $0.5\% < \frac{\delta_f}{R_s} < 5\%$. Considering that the coarse frequency offset estimation leads to a residual offset ϵ_c, its fine estimation error is $\epsilon_f = |\tilde{\nu} - \epsilon_c|$. The value of ϵ_f gives the residual frequency offset after *INITIALIZATION STEP*. In Figure 7, the performance of coarse and fine estimation during *INITIALIZATION STEP* is illustrated as a function of the SNR, considering two IBO values in saturation regime, 1dB and 7dB. The frequency offset correction performance during *TRACKING STEP* is characterized with a 30KHz/s drift. Regardless of the IBO considered, the coarse frequency estimation is sufficient when SNR is over 9dB. The difference between IBO of 1dB and 7dB shows off the robustness of the method in the saturation regime.

B. Receivers performances

The two proposed schemes for the sampling offset issue can be compared through their detection performance by observing the bit error rate (BER) achieved by
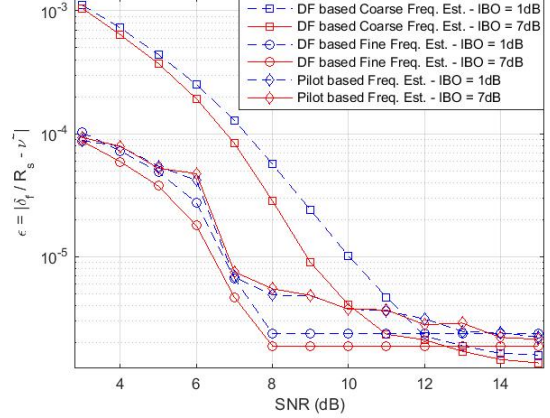

Fig. 7. Mean Residual Frequency Offset ϵ as a function of SNR for IBO = 1dB/7dB - $\alpha = 0.7$, $\beta = 0.1$ - Monte-Carlo on 1000 Dummy Frames and/or 1000 Pilots sequences.

both schemes. As a benchmark, the ideal synchronization performance is considered too in Figure 9. In the same transmission channel ($\alpha = 0.7$, $\beta = 0.1$ and IBO=3dB). We consider $BPSK$, $QPSK$ and $8PSK$ modulations, depicting performance in different SNR ranges with a coding rate $\rho = 2/3$. In Figure 3, the turbo-equalization scheme implemented is depicted. The detection consists in 3 turbo-iterations between the MAP detector and the LDPC decoder. During the first turbo-iteration, 5 decoding iterations are applied, during the second one, 10 decoding iterations and finally 15 decoding iterations during the 3rd turbo-iteration.

The performance of scheme A shows off that the Nyquist sampling instant is no more critical when FTN signaling is considered in the saturation regime. Its performance is only 0.2 dB beyond the ideally synchronized detection when BPSK and QPSK are considered and 0.3dB when 8PSK is considered. For the scheme B, the performance is satisfying too, achieving detection 0.3dB and 0.4dB beyond the ideal synchronization scenario. The loss is partly due to the phase noise ϕ_k since the correction applied on time offset and frequency offset ensures a well performing detection.

V. CONCLUSION

In this paper, the synchronization issue for FTN signaling in non-linear channel has been addressed with frame structures compliant with the DVB-S2X requirements. Volterra series paired with channel estimation based on known sequences leaded to two schemes, A and B. Both offer interesting performance regarding their feasibility, even considering the worst case : Strong ISI context (IBO=1dB) and low SNR (SNR=3dB) over the downlink. With respect to an ideal synchronized transmission, both scheme introduce a weak loss between 0.2dB (Scheme A) and 0.3dB (Scheme B) on
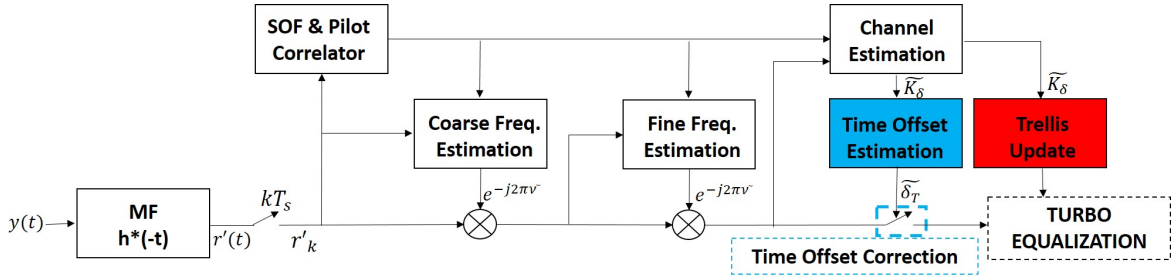
Fig. 8. Scheme A (red) and Scheme B (blue).

the SNR for detection. The performance of scheme A underlines an interesting point: the Nyquist optimal sampling instant does not stand when FTN signaling is considered in saturation regime. Moreover, when Scheme B is implemented, the channel estimation paired with trellis update is interesting considering the payload aging process which makes the channel model slowly varying in time. Considering the results in this paper and the fact that future satellite communications will require advanced receivers, FTN signaling in the saturation regime could be a strong candidate for spectral efficiency improvement in future standardization. In further studies, FTN signaling in wideband satellite communications scenario will be addressed and advanced predistorder paired with FTN transmission will be considered.
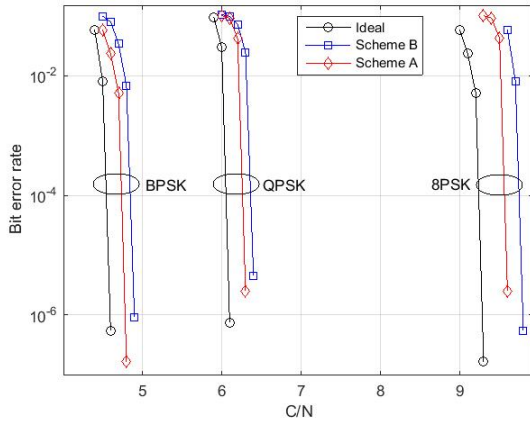

Fig. 9. BER Vs SNR for BPSK(L=7), QPSK(L=7) and 8PSK(L=5) - $\alpha = 0.7$, $\beta = 0.1$ and IBO=3dB.

REFERENCES

[1] J.E. Mazo, "Faster than Nyquist Signaling" Bell Syst. Tech. J., vol. 54, pp, 1451-1462, Oct. 1975.
[2] A. D. Liveris, C. N. Georghiades, "Exploiting Faster-Than-Nyquist Signaling" IEEE Transactions on Communications, Vol. 51, No. 9, Sept. 2003
[3] F. Rusek and J. B. Anderson, "Constrained capacities for faster than Nyquist signaling", IEEE Trans. Inf. Theory, vol. 55, no. 2, pp. 764-775, Feb. 2009.
[4] N. Pham, J. B. Anderson, F. Rusek and J. M. Freixe , "Exploring Faster-than-Nyquist for Satellite Direct Broadcasting", 31st AIAA International Communications Satellite Systems Conference, 2013

[5] S. Benedetto, E. Biglieri, and R. Daffara, Modeling and performance evaluation of nonlinear satellite links-a volterra series approach, IEEE Transactions on Aerospace and Electronic Systems, vol. AES-15, no. 4, pp. 494 507, july 1979
[6] . G. Colavolpe, A. Piemontese, "Novel SISO Detection Algorithms for Nonlinear Satellite Channels", IEEE Wireless Cmmunications Letters, Feb. 2012.
[7] A. Ugolini, A. Modenini, G. Colavolpe, "Advanced Techniques for Spectrally Efficient DVB-S2X Systems ", 7th Advanced Satellite Multimedia Systems Conference and the 13th Signal Processing for Space Communications Workshop (ASMS/SPSC), 2014
[8] J.A. Lucciardi, N. Thomas, M.L. Boucheret, C. Poulliat, G. Mesnager, "Trade-Off Between Spectral Efficiency Increase and PAPR Reduction When Using FTN Signaling: Impact Of Non Linearities" IEEE International Conference on Communications (ICC), 2016
[9] E. Casini et al., "DVB-S2 modem algorithms design and performance over typical satellite channels" International Journal on Satellite Communication Networks, vol. 22, no 3, Jun. 2004
[10] P. Kim, D.-G. Oh, "Synchronization for Faster Than Nyquist Signalling Transmission" IEEE International Conference on Ubiquitous and Future Networks (ICUFN), 2015
[11] X. Liang, A. Liu, H. Wang, K. Wang, S. Peng, "Method of NDA Frequency-offset Estimation for Faster-than-Nyquist Signaling with High-order Modulation" IEEE International Conference on Communications in China (ICCC), 2016
[12] ETSI, Digital Video Broadcasting (DVB): Second generation framing structure, channel coding and modulation systems from Broadcasting, Interactive Services, News Gathering and other broadband satellite applications. Part 2: DVB-S2 Extensions (DVB-S2X), ETSI EN 302 307-2 V1.1.1, 10/2014
[13] ETSI, Digital Video Broadcasting (DVB): Implementation guidelines for the second generation system for Broadcasting, Interactive Services, News Gathering and other broadband satellite applications, Part 2 - S2 Extensions (DVB-S2X), A171-2, 03/2015
[14] D. R. Morgan, Z. Ma, J. Kim, M. G. Zierdt, J. Pastalan, "A Generalized Memory Polynomial Model for Digital Predistortion of RF Power Amplifiers" IEEE Transactions on Signal Processing, vol. 54, no 10, Oct 2006
[15] M. Morelli, U. Mengali, Carrier-Frequency Estimation for Transmissions over Selective Channels, IEEE Transactions on Communications, vol. 48, no 9, Sep. 2000
[16] G. Ungerboeck, "Adaptive Maximum-Likelihood Receiver for Carrier-Modulated Data-Transmission Systems", IEEE Transactions on Communications, vol. COM-22, No. 5, May 1974
[17] G. David Forney, "Maximum-Likelihood Sequence Estimation of Digital Sequences in the Presence of Intersymbol Interference ", IEEE Transactions on Information Theory, vol. IT-18, No. 3, May 1972
[18] L. R. Bahl, J. Cocke, F. Jelinek, and J. Raviv , "Optimal Decoding of Linear Codes for Minimizing Symbol Error Rate", IEEE Transactions on Information Theory, March 1974
[19] Adel A. M. Saleh, "Frequency-Independent and Frequency-Dependent Nonlinear Models of TWT Amplifiers", Senior Member IEEE, IEEE Transactions on Communications, vol. com-29, No. 11, Nov. 1981